Radiation Measurements in the FLASH Tunnel in Summer 2006

Roger José Hernández Pinto, Martin Otto, Manfred Valentan

DESY-Note-2006-04

Supervisor: Bhaskar Mukherjee

Editor: Markus Hoffmann

December 26, 2006

This paper reports about the investigation of the radiation dose coming from the superconducting cavities due to dark current and field emission in the FLASH tunnel, which where done by the summer students from the DESY Summer Student Program 2006.

Contents

1 Introduction

Once particles are accelerated and/or high fields are applied the cavity material is beeing stressed in many ways, of which more than one results in secondary (radioactive) radiation. E.g. due to field emission particles are extraced from the cavity walls. This effect appears at gradients higher than $5000\frac{\mathrm{MV}}{\mathrm{m}}$, and especially occurs even without main electron beam. Since the highest gradients applied at FLASH are $30\frac{\mathrm{MV}}{\mathrm{m}}$, one could think that field emission would be a negligable effect.

But the real problem here are inhomogenities on the surface of the internal wall of the cavity. Once only a few atoms will stand out, the field lines will concentrate there and the effective field tremendously increases, exceeding the threshold. These inhomogenities can not be avoided and thus there will always be field emission, especially reaching higher and higher accelerating gradients. Thus there is an energy loss while applying an accelerating field, namely a little fraction of the energy may be lost in any device, due to leakage or ionising radiation.

Not only particles coming from the cavity walls, but also field emitted particles from the electron gun are accelerated. This effect is called dark current. The dark current creates much higher radiation doses all over the tunnel, due to uncontrolled particles reaching high energies. But this can be avoided via a collimator behind the gun. Keep in mind that the beam does not necesarily need to be in operation for dark current to occur. Once these particles will hit the cavity wall high energetic gamma photons and photo neutrons are produced. Another reason for high energetic radioactive radiation can originate from rest gas ionisation inside the beam line and cavities.

These stray mixed neutron-gamma radiation field usually triggers the malfunction of a semiconductor based microelectronic and photonic devices situated in the vicinity of the accelerator facility. Hence, the characeristics of this radiation field must be well known in order to quantify the magnitude and time-scale of radiation effects in semiconductors. Thus one has to deal with (and measure!) high energetic gamma radiation and so-called photo neutrons, with occurring doses which will be essential to interpretate radiation effects on microelectronic devices operating close to the accelerating structures. For a short summary of radiation types and effects on electronics see figure 1.

On the one hand one does not want to expose the electronics to the radiation field and therefore has to protect them, but on the other hand, for better control properties, like short cable lengths and calculation times for high beam stability, one wants to have them as close as possible. This decision still has to be made on the XFEL and ICL designs.

Thus we were participating in a series of radiation measurements serving the purose to better estimate a typical radiation dose, and dark currents during high gradiant operation. In the following different dosimeters are shortly introduced and a program will be superficially described which was a first approach to estimate a response matrix for calculating the radiation dose coming from the cavities via a given genetic algorithm, which unfolds the measured spectrum.

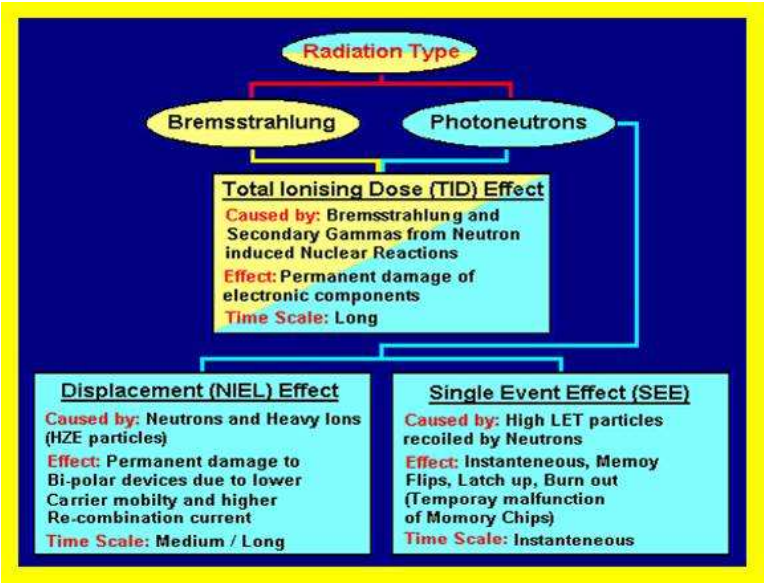

Figure 1: Radiation types and effects on electronics

2 Dosimetry

Dosimetry is the measurement of absorbed dose in matter and tissue resulting from the exposure to ionizing radiations.

Doses are measured in gray (Gy) for matter or sieverts (Sv) for biological tissue, where 1 Gy or Sv$= 1$ Joule/kilogram. Unfortunately, non-SI units are still somewhat prevalent in this field, thus dose is measured in rad and dose equivalent in rem (100 rad $= 1$ Gy and 100 rem $= 1$ Sv). The dose refers to the amount of energy or damage deposited in matter.

The worldwide average background dose for a human being is about 3.5 mSv per year, mostly from cosmic radiation and natural isotopes in the earth. Workers who deal with radioactive substances or might be exposed to ionising radiation carry personal dosimeters, they are so called 'controlled persons'. These dosimeters contain materials that can be used in thermoluminescent dosimetry (TLD) or optically stimulated luminescence (OSL). During our work we had to enter the FLASH tunnel, and thus were considered controlled persons. For controlled persons in Germany the limit dose per year is 20 mSv, in the USA it's 50 mSv. To monitor this, we all had personal dosimeters, which we had to wear each time we entered the tunnel.

2.1 Radiochromic film

Radiochromic dosimetry detector foils are thin foils of a gamma (or particle radiation) sensitive material. It is transparent before exposure to radiation, and develops a gray to blue colour

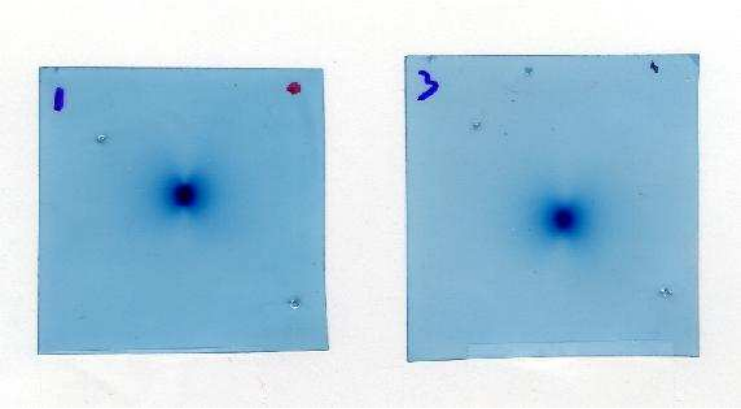

Figure 2: Radiochromic foils, irradiated at one spot

after exposure. The colour intensity is a function of the radiation exposure; higher exposures result in progressively darker colour. This colour change can be accurately measured to determine absorbed dose using any device that measures optical density or absorbance. In our case we used a red LED and measured the absorbance with reference to an unirradiated foil. From the calibration measurement, where several foils were irradiated with different doses, one can determine the suffered dose.

The foils may be used over a wide-range of absorbed doses. Radiochromic foils have low sensitivity to ambient room light, which simplifies handling procedures and enhances image stability. The foils can easily be cut by hand, giving them any size and shape desired.

2.2 TLD

The thermoluminescent dosimeter (TLD) can be used to measure ionising particles. A thermoluminescent material, that is exposed to radiation for a certain time, will emit visible light when it is externally, thermally excited. The amount of light measured while heating is then directly proportional to the collected dose of the probe device. The energy from heating will be stored in electronic metastable states, that than emit the light, and thus the wavelenth depends on the material one chooses (e.g. LiF, CaF, or AlO).

A TLD and a measuring station is shown in figure 3.

Some util properties are high sensitivity, a relativly wide energy range, and the small size of the probe, besides some more. E.g. recorded signals can be stored over a long time, due to low fading, but this effect is temperature dependent.

Since thermoluminescence is a relative measurement method, it is necessary to calibrate the dosimeter in order to obtain absolute values, which is a quiet complex method, and will not be explained here.

Figure 3: TLD and measuring station

2.3 Bubble Dosimeter

Bubble detectors provide instant visible detection and measurement of neutron dose. Inside the detector tiny droplets of superheated liquid are dispersed throughout a clear polymer. When a neutron strikes a droplet, the droplet inmediately vaporizes, forming a visible gas bubble trapped in the gel. The number of droplets provides a direct measurement of the tissue-equivalent neutron dose.

The bubble detector is the only neutron dosimeter for which the response is independent of dose rate and energy, with zero sensitivity to gamma radiation. Bubble detectors are so compact, lightweight and rugged, that they can be clipped to a coat or shirt pocket, placed in areas with limited access, or used in close proximity to a neutron source with a quick assessment. With an isotropic angular response, neutron dose can be accurately measured regardless of the direction of neutrons relative to the detector.

2.4 LEDs

In addition to the devices described above, also LEDs[1] are used to measure neutron doses. The light yield of irradiated LEDs drops as a function of the suffered dose. When the space charge zone of the diode is damaged by ionizing radiation, recombination centers are produced. Due to that only a fraction of the electron/hole pairs undergo radiative recombination, emitting light. The rest is dissipated in the space charge zone by non radiative recombination, they are catched by the recombination centers.

[1] LED: Light Emitting Diode

Figure 4: Picture of a bubble dosimeter; the upper one is irradiated and bubbles have formed.

After a calibration measurement, similar to the calibration of radiochromic foils, the dose can be derived by measuring the light yield with a light sensitive device.

Since LEDs are very cheap, precisely manufactured and available in huge quantity, they are an interesting alternative to other measuring principles, but there is one reasonable drawback. LEDs do not have a high sensitivity, so one can't use them to measure low doses, only application in strongly radiating environment makes sense.

2.5 RADMON

The RADMON[1] is a permanent radiation measuring device installed in the FLASH tunnel. In principle it is nothing more than a SRAM chip and a readout system. Ionizing particle radiation, in our case mainly neutrons, are able to interact with the chip material, dposite energy, and thus cause a bit to flip. This is called 'Single Event Upset' (SEU). Said radiation monitoring system permanently reads out the SRAM and compares the current bit configuration with the previous one. When they differ, a SEU has occured and is recorded. The SEU history can be viewed via the internet, using the url:

`http://neo.dmcs.p.lodz.pl:9998/`

In figure 6 one can see a RADMON system next to the wall (the SRAM chip is located inside the white 'sphere'), in front of the accelerator module.
A little anecdote: Since the probability for SEUs increases with the bit density of the SRAM,

[1] short for RADiation MONitor

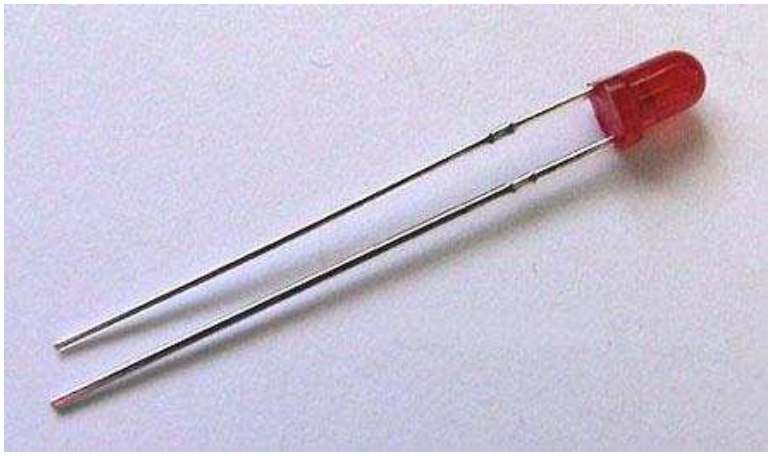

Figure 5: Light emitting diode

one expected better results with newer chips. Everyone was surprised when suddenly the opposite occured. After some search one found out, that the manufacturers of these chips with high bit density already had problems with SEUs caused by muons coming from cosmic radiation. So there is a built-in radiation shielding implemented, which makes these chips unusable for radiation detection. Unfortunately nowadays all chips are produced using this technique, and so one can hardly find suitable hardware.

3 The experiment

In order to investigate the radiation dose coming from the superconducting cavities due to dark current and field emission we installed the in section 2 described dosimeters in the FLASH tunnel, supervised by Dr. Bhaskar Mukherjee. We used TLDs, Bubble dosimeters and radiochromic foils as well as LEDs. The measurement was performed by distributing several dosimeters over the cryomodules 4 and 5 of the FLASH linear accelerator (see the sketch in figure 7). To do this, we fixed the devices on cords. Altogether we prepared 16 of these cords to perform two measurements, one from monday, 7^{th} of august to tuesday, 8^{th} of august, and the second one from said tuesday to wednesday, 9^{th} of august 2006.

Since every cryomodule consists of eight cavities we could not instrument every cavity with detectors, but every second. So we installed, tieing the cords around the cryomodule, eight Bubble dosimeters and eight TLDs, each on top of the module, and 16 radiochromic foils, eight on top and eight on bottom of the module (see figure 8). In addition to that we equipped the power couplers[1] of every cavity with two radiochromic foils each, every time putting a high sensitive and a low sensitive one (see figure 9). LEDs were mounted directly onto the beam pipe, just on the pipe going into module 4 and on the one coming out of module 5.

[1]The radio frequency is fed into the cavities via the power couplers

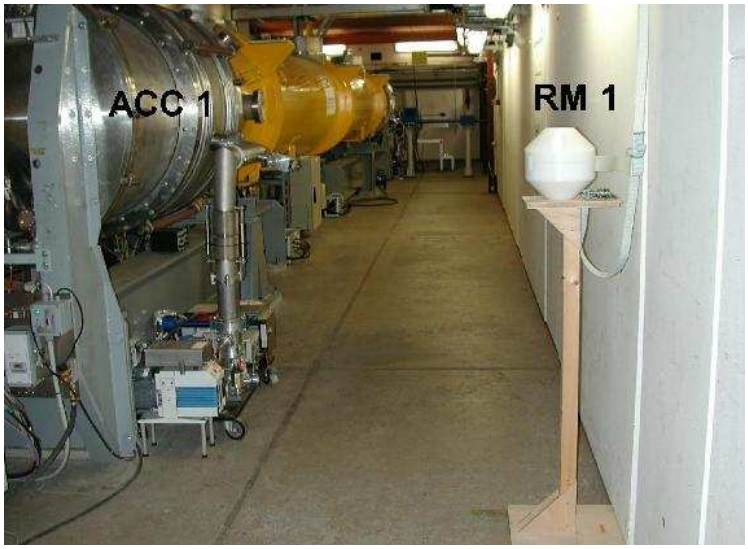

Figure 6: RADMON system

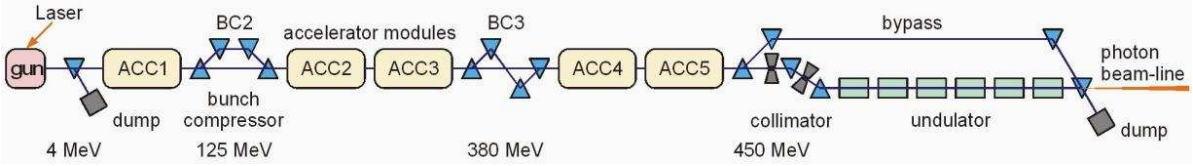

Figure 7: The FLASH facility.

The detectors were exposed over night, and the next day replaced for the second measurement. All relevant data for the measurement series is summarized in table 1.

4 Evaluation

First, the suffered dose of every detector has to be determined.

The TLDs are read out using a special device, which heats up the TLDs and measures the light emitted. Radiochromic films are evaluated by illuminating them with a red LED, measuring the light transmitted. The dose can be determined from the calibration curve. LEDs are analyzed in a similar way.

The evaluation of the suffered dose of bubble dosimeters is much more exhausting, since the number of bubbles had to be counted by hand. But once the number is known, the dose can be derived using the calibration curve.

Since each of these detectors measures the integrated dose, summing up the radiation from all directions, one can not easily tell which cavity radiates which dose. The situation can be

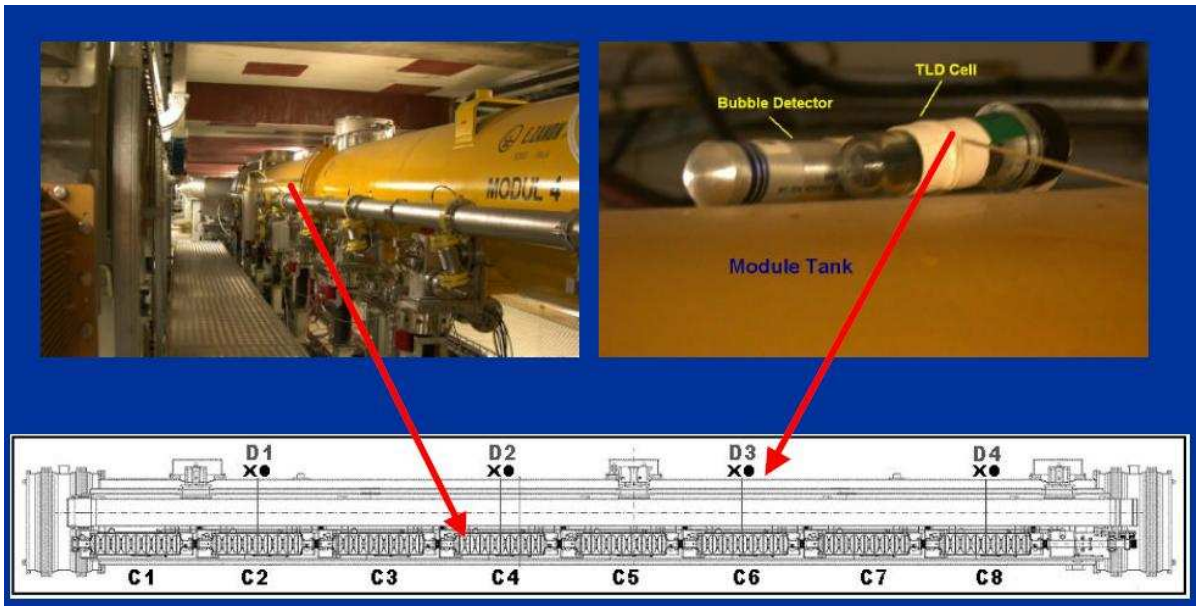

Figure 8: Detectors tied to module.

written in form of a set of equations, using a matrix representation.

$$\begin{bmatrix} \Phi_1 \\ \vdots \\ \Phi_m \end{bmatrix} = \begin{bmatrix} A_{1,1} & \dots & A_{1,n} \\ \vdots & \ddots & \vdots \\ A_{m,1} & \dots & A_{m,n} \end{bmatrix} \cdot \begin{bmatrix} \Psi_1 \\ \vdots \\ \Psi_n \end{bmatrix} \tag{1}$$

The column vector on the left hand side of the equation represents the measured doses, whereas the vector on the right hand side of the equal sign represents the dose coming from each cavity. The matrix, that connects these two vectors is called 'response matrix'. It describes the mixing of the emitted doses from all different cavities arriving at the different detectors, taking into account screening and distance effects. For a graphical representation of this context see figure 10.

The vector of the emitted doses is unknown and one wants to derive it. The set of equations can't be solved exactly, since the response matrix is not quadratic. And even if it were quadratic there would exist an infinite manyfold of solutions. Therefore one needs a way to find the solution vector, that fits the measured data best. This is called 'Unfolding'. The technique we used was a so called Genetic Algorithm.

5 Unfolding using a Genetic Algorithm (GA)

The GA is a stochastic global search method that mimics the metaphor of natural biological evolution. GAs operate on a population of potential solutions applying the principle of survival

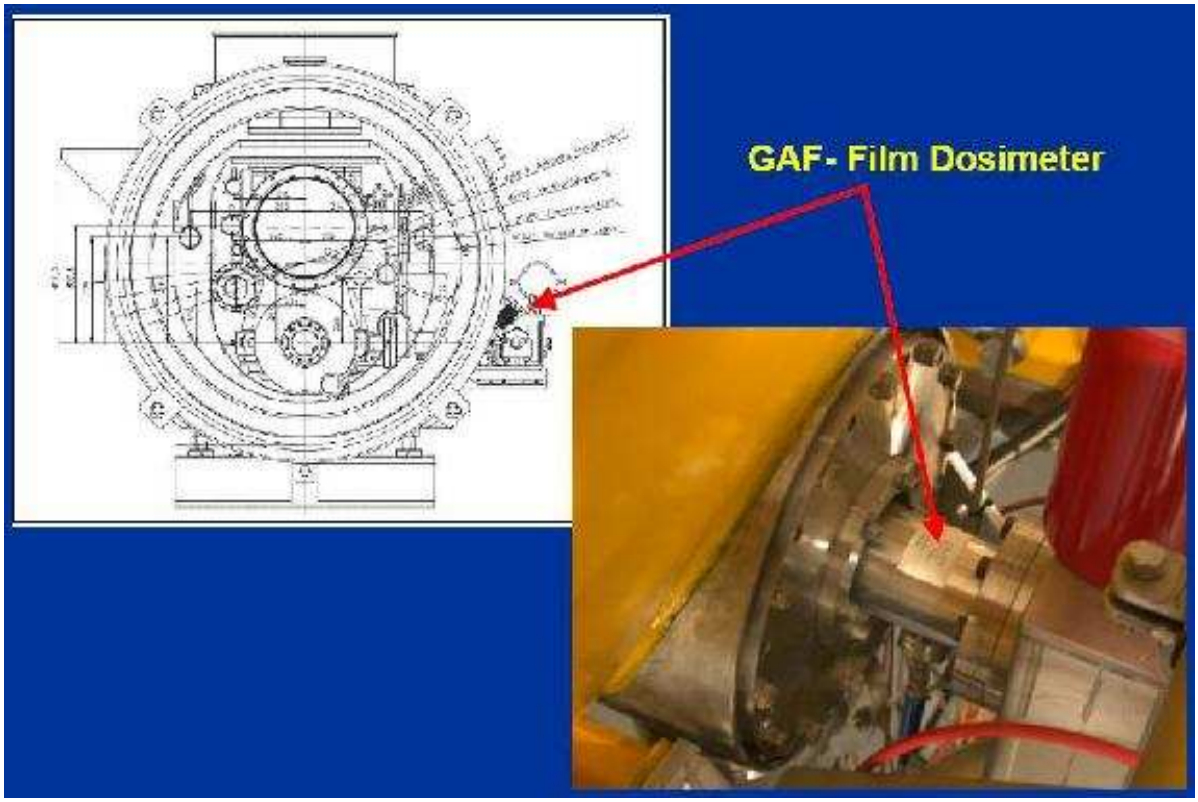

Figure 9: Detectors at power couplers.

Series:	$1^{st}, 7^{th} - 8^{th}$of august 2006	$2^{nd}, 8^{th} - 9^{th}$of august 2006
RF-Gun Status:	OFF	OFF
Duty Cycle (Rep rate):	10 Hz	10 Hz
Start:	16:00 hr	11:00 hr
Stop:	9:30 hr	14:10 hr
Exposure Duration:	17h 30min	26h 10min
Gradient (ACC4):	$\approx 22\frac{\mathrm{MV}}{\mathrm{m}}$	$\approx 14\frac{\mathrm{MV}}{\mathrm{m}}$
Gradient (ACC5):	$\approx 22.5\frac{\mathrm{MV}}{\mathrm{m}}$	$\approx 30\frac{\mathrm{MV}}{\mathrm{m}}$
Cavity Status:	All cavities in operation	All cavities in operation

Table 1: Radiation measurement, relevant data

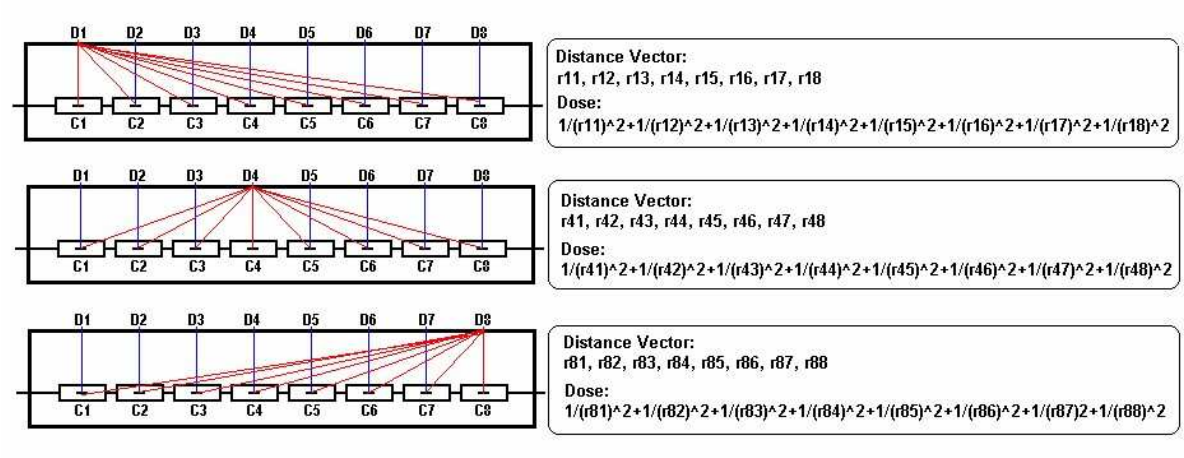

Figure 10: Concept of response matrix.

of the fittest to produce (hopefully) better and better approximations to a solution. At each generation, a new set of approximations is created by the process of selecting individuals according to their level of fitness in the problem domain and breeding them together using operators borrowed from natural genetics. This process leads to the evolution of populations of individuals that are better suited to their environment than the individuals that they were created from, just as in natural adaptation.

Step 1: create an initial population of randomly derived solutions.
One advantage of a GA is, that no estimate of the solution is neccesary to start from. The first generation of individuals is created randomly.

Step 2: find the best fitting individuals in the population.
During the reproduction phase, each individual is assigned a fitness value derived from its raw performance measure given by the objective function. In our case, the individual is multiplied by the response matrix, and afterwards a fitness value (comparable to a root mean square) for the deviation from the real measured vector is calculated. This value is used in the selection to bias towards more fit individuals. Highly fit individuals, relative to the whole population, have a high probability of being selected for mating whereas less fit individuals have a correspondingly low probability of being selected.

Step 3: breed together the best fitting individuals.
Once the individuals have been assigned a fitness value, they can be chosen from the population, with a probability according to their relative fitness, and recombined to produce the next generation.

Step 4: mutate the new generation.
A further genetic operation, the mutation, is then applied to the new generation, again

with a set probability. Mutation causes the individual genetic representation to be changed according to some probabilistic rule.

Step 5: repeat the steps 2 to 4.
This has the effect of tending to inhibit the possibility of converging to a local optimum, rather than the global optimum. After recombination and mutation, the individuals again are assigned a fitness value and are selected for mating according to their fitness, and so the process continues through subsequent generations. In this way, the average performance of individuals in a population is expected to increase, as good individuals are preserved and bred with one another whereas the less fit individuals die out.

Step 6: stop the process, when certain criteria are satisfied.
The GA is terminated when some criteria are satisfied, e.g. a certain number of generations, a mean deviation in the population, or when a particular point in the search space is encountered.

Running through these steps, the GA is able to solve multidimensional inverse optimization problems and yields the best solution for a global minimum of the objective function.

With help of a genetic algorithm we tried to find out the dose radiated by each cavity (see also [1]). To do this, we assumed the points, where the radiation comes from, to be in the center of the cavity. We called these points the 'expansion points' for the unfolding procedure. To be precise, radiation is assumed to come from the beam axis, from the center of the fifth cell of each cavity. With these assumptions we know the whole geometry of the experiment and can calculate the response matrix, that links the radiation of the cavities and the dose measured by our detectors.

6 Calculating the response matrix

The response matrix takes into account the weakening of the radiation due to the distance between source and detector and the absorption in shielding material. The intensity of the radiation drops proportional to

$$\Delta I \propto 1/r^2 \tag{2}$$

where r is the distance between the radiation source and the detector.

The attenuation delivers an additional factor of

$$\Delta I \propto 2^{-\mu \cdot d_{\text{eff}}} \tag{3}$$

μ is the attenuation coefficient of the shielding material and d_{eff} is the effective thickness of material traversed, taking into account the angle between the surface orientation and the direction of radiation. After travelling a distance of $1/\mu$ through the material the intensity has dropped to one half of the initial one.

In order to have the possibility to calculate response matrices for any set of expansion points and detector positions, we developed a litte program, that does the work for us.

This little routine provides the possibility to choose any number of arbitrary expansion points inside a cylindrical steel shield of freely selectable radius, thickness and attenuation coefficient. Moreover one can choose any number of arbitrary detector positions outside the shield. Using these input data the program calculates the correct matrix element for every direct line from each expansion point to each detector.

The consideration of equation (2) is easy, one only has to calculate the absolute distance between the current expansion point and the current detector position. The $1/r^2$ law describes the dropping of the flux density of particle radiation. It can easily be understood when one takes into account that we assume a pointlike source. If we would instrument the whole space angle 4π, we would measure every particle radiated by the source. Since spherical surfaces grow proportional to r^2, the flux density drops proportional to $1/r^2$. That leads us to the problem, that we can't derive the flux density of the source, because we assumed it to be pointlike. Therefore we calculate the flux density at a given reference radius rear the source. In our case this reference radius was chosen to be 1 cm. The flux density at the reference radius can be calculated, using said law, like this:

$$f_{ref} = r^2_{detector}/r^2_{ref} \cdot f_{detector} \tag{4}$$

Thus, the matrix element has the form

$$f_{\mathrm{detector(i)}} = \frac{r^2_{\mathrm{ref(j)}}}{r^2_{\mathrm{detector(i)}}} \cdot f_{\mathrm{ref(j)}} = \frac{(0.01\mathrm{m})^2}{r^2_{\mathrm{detector(i)}}} \cdot f_{\mathrm{ref(j)}} \tag{5}$$

Due to this we have to consider an additional factor $(0.01m)^2$.

Considering equation 3 is more difficult, since one has to calculate the cosine of the angle between the difference vector (between the expansion points and the detector positions) and the normal vector of the perpendicular plane in the intersection point. This is done by the MATLAB function 'costheta.m'. As an input it accepts either a pair of vectors (defining expansion and detector point), a list of pairs of vectors (here the cosine is calculated for every pair of vectors seperately), one vector defining the expansion point and a list of detector coordinates (calculating the connection between this expansion point and every detector point) or vice versa with a list of expansion points and one detector point. Furthermore, since the angle between the difference vector and the normal vector is dependent on the radius of the cylinder surface, the radius has to be put in, too.
Once the cosine of this angle is calculated, the effective thickness the radiation 'sees' is calculated according to

$$d_{\mathrm{eff}} = d/cos(\theta) \quad . \tag{6}$$

With these ingrediences the response matrix can easily be calculated.

Figures 11 and 12 show a three dimensional and a two dimensional representation of an example response matrix. Considering the logarithmic scale, one can see, that expansion

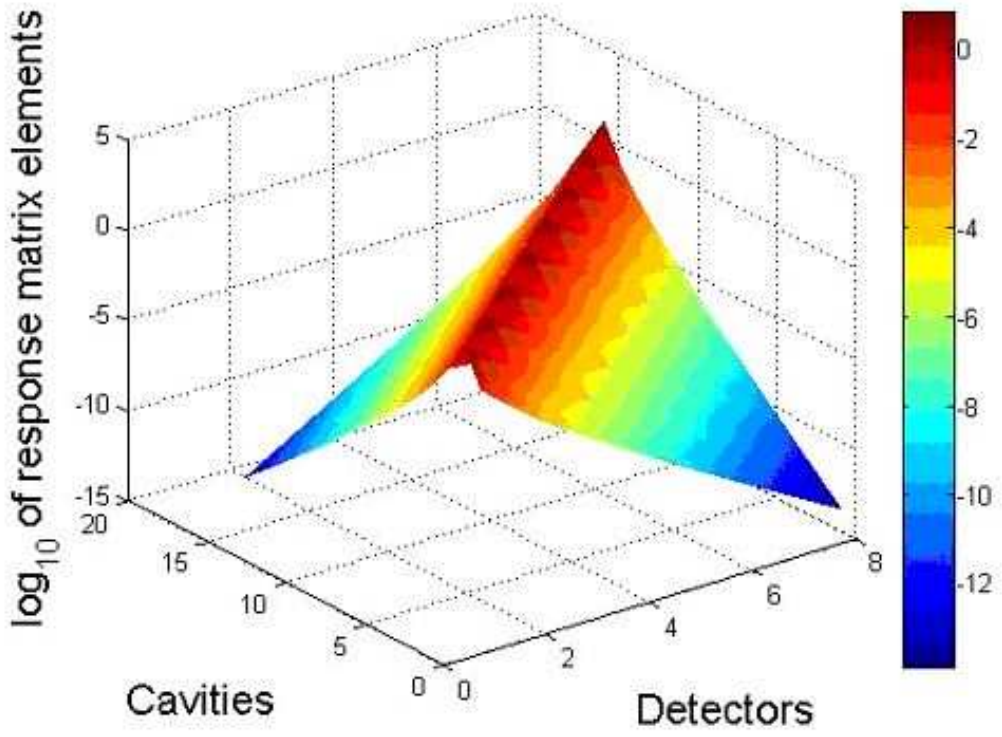

Figure 11: 3D matrix representation.

points far away from detector points hardly contribute. In principle, this promises a good discrimination of the doses radiated by different cavities.

7 Results

We have explicitly evaluated the gamma and neutron dose rates near the ACC 4 and ACC 5 modules produced by cavity field emission (figures 13 and 14). The gamma dose rates were found to be two orders of magnitude higher than the neutron dose rates. Both gamma and neutron dose rates rise exponentially with the increment of the module gradient.

We also have evaluated the gamma dose rate at every power coupler of both modules using radiochromic films (figure 15).

The radiation field emitted by each of the eight cavities per module was unfolded using the readings of the eight TLD gamma detector (inverse calculation). Unfortunately the result of the unfolding was not satisfying, although the unfolded cavity doses could very precisely explain the measured doses. Our assumption is, that one can't describe the radiation properties of the cavities by simply assuming all the radiation coming from the middle. This violently

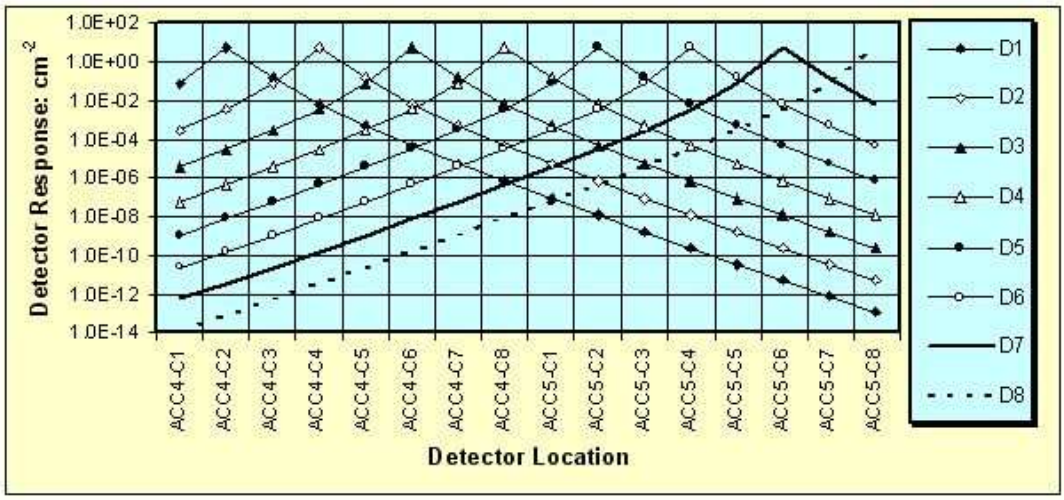

Figure 12: 2D matrix representation.

simplified model is too simple. In reality the radiation source isn't located on the beam axis, but comes from the surface of the cavity, moreover the whole nine celles radiate, not only the center cell of a cavity alone.

Since we have only eight detector points for 16 cavities, an unfolding procedure using more than one expansion point per cavity would not yield good results. But recently another measurement with 38 radiochromic foils is done, and we hope that with these data an unfolding will give us reliable and satisfying results.

As a further outlook to this topic we can say that the whole comunity (of XFEL as well as ILC) are highly interested in this type of radiation dose estimation in order to be able to plan correctly and finally decide where all the control parts will go (either inside or outside the tunnel). This will imply different reqirements for the system, such as "will there be two or only one tunnel?" and "If electronic systems are placed in the direct vicinity of the beam line how good will it have to be protected against radiation?". Thus like in our feedback loop one thing affects the next and answers to questions always leed to new questions...

8 Acknowledgements

The summer student program was a great opportunity for us to get an impression how DESY works, and how work at DESY lookes like. We thank our supervisor Dr. Simrock for integrating us as regular coworkers into the group of MSK. Also we like to say thanks to Markus Hoffmann, from whom we really learned a lot about the busines. A special thanks goes to Bhaskar Mukherjee for giving us in sights to the FLASH facility, and demanded us to contribute ideas to his project. Furthermore we thank Matthias Hoffmann, Waldemar Koprek, Karol Suchecki and Wojciech Giergusiewicz for the direct support in every question on our

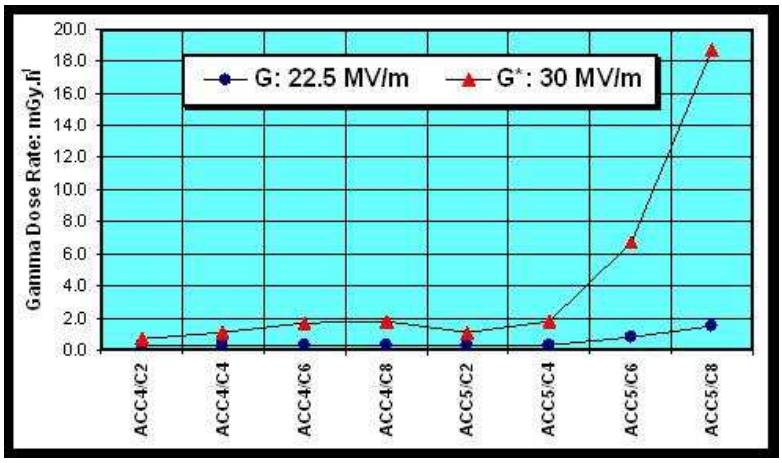

Figure 13: Gamma dose rate.

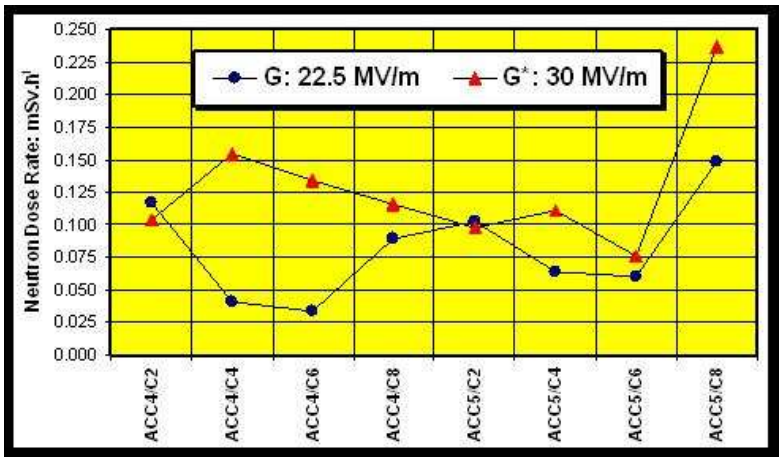

Figure 14: Neutron dose rate.

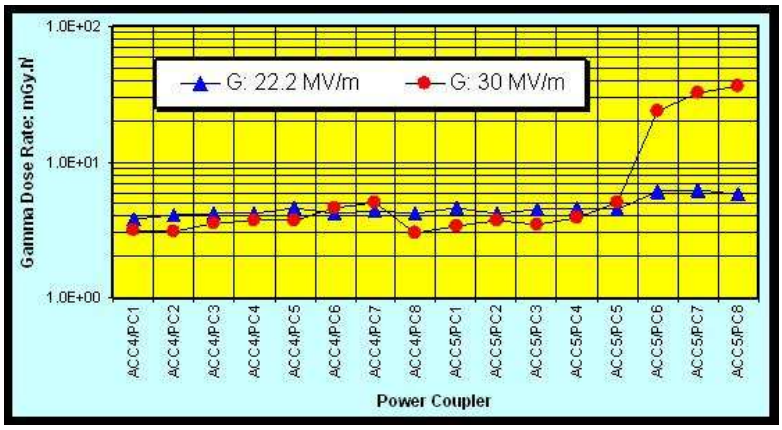

Figure 15: Gamma dose rate at power couplers.

projects. Last but not least we thank the organisators and all Summies 2006 for lots of fun, the great summer, and a good time at DESY.

References

[1] Bhaskar Mukherjee, *A Genetic Algorithm Tool for the Analysis of Activation Detector Data to Unfold High-Energy Neutron Spectra*, Radiation Protection Dosimetry Vol. 110, Nos 1-4; pp. 249–254, (2004)

[2] Bhaskar Mukherjee et al., *Dosimetry of high-energy electron linac produced photoneutrons and the bremsstrahlung gamma-rays using TLD-500 and TLD-700 dosimeter pairs*, Nuclear Instruments and Methods in Physics Research A 545, pp. 830-841, (2005)

[3] D. Makowski et al., *SEE induced in SRAM operating in a superconducting electron linear accelerator environment*, 2005 NSTI, Nanotechnology Conference and Trade Show, Nanotech, March 2005, San Francisco, USA.

[4] D. Makowski et al., *SRAM based passive dosimeter for accelerator environment*, 7th European Workshop on Diagnostics and Instrumentation for Particle Accelerators, DIPAC2005, June 2005, Lyon, France.

[5] D. Makowski et al., *Radiation tolerant system for neutrons fluence measurement*, MIXDES2005, June 2005, Krakow, Poland.

[6] B. Mukherjee et al. *Interpretation of the single event upset in static random access memory chips induced by low energy neutrons*, MIXDES2005, June 2005, Krakow, Poland.

[7] B. Mukherjee et al., *A neutron irradiation device for the testing of microelectronic components to be used in the radiation environment of high-energy particle accelerators at DESY*, MIXDES2005, June 2005, Krakow, Poland.

[8] B. Mukherjee, *Radiation effects on electronics operating in the high energy electron linac environments at DESY*, (invited lecture), IEEE SPIE Workshop, August 2005, Warsaw, Poland.